Kinetic Analysis of Two Hyperbranched $A_2 + B_3$ Polycondensation Reactions by NMR Spectroscopy

Andreas Reisch,† Hartmut Komber,* and Brigitte Voit‡

Leibniz Institut für Polymerforschung Dresden, e.V., Hohe Strasse 6, 01069 Dresden, Germany

Received April 5, 2007; Revised Manuscript Received July 12, 2007

ABSTRACT: The kinetics of the polycondensation of A_2 and B_3 monomers leading to hyperbranched polyesters was studied by NMR spectroscopy and compared with theoretical predictions. Combinations of two different A_2 monomers, the aromatic terephthaloyl chloride (TCl, A_2) and the aliphatic adipic acid (AA, A_2), respectively, with 1,1,1-tris(4-trimethylsiloxyphenyl)ethane (TMS−THPE, B_3) and 1,1,1-tris(4-hydroxyphenyl)ethane (THPE, B_3), respectively, were studied in different molar ratios of the monomers. On the basis of a complete ^{1}H and ^{13}C NMR signal assignment for the structural units of the two resulting hyperbranched polymers their relative concentration as a function of conversion was determined. In the case of TCl/TMS−THPE, the degree of branching just before gelation increased with increasing A_2 content. A further increase of DB could be obtained by sequential addition of the $A_2 + B_3$ monomer mixture. Since the kinetic data for that system did not describe the development of structural units expected for equal and independent reactivity of the functional groups (ideal case), the relative rate constants of the basic reaction steps were determined by simulation to fit best the experimental data. A decrease of the reactivity of the second A function after reaction of the first and a small increase of the reactivity of B functions after reactions of other B groups in the molecule were found. The kinetic data for the less reactive system AA/THPE, however, followed the development expected for an ideal polymerization even though very long reaction times had to be applied at high reaction temperature which favored side reactions.

Introduction

During the last 2 decades, dendrimers and hyperbranched polymers have drawn great attention due to their globular shape resulting from the branch on branch topology and their unique properties.[1−6] Hyperbranched polymers are of special interest as their easy synthetic accessibility, typically by one pot syntheses, allows for their production in large quantities and their application on an industrial scale. Among the different synthetic approaches the predominant one is polycondensation,[7,8] others being, e.g., self-condensing vinyl polymerization (SCVP)[9] and ring-opening multibranching polymerization.[10−12] The preferred method is the polymerization of AB_n type monomers ($n > 1$; most $n = 2$) which has the advantage that under optimal conditions gelation is virtually absent in the system.[13] If the required AB_n monomer is not accessible or not stable enough, the $A_2 + B_3$ approach may be used. As in those systems gelation occurs at higher conversion, the reaction has to be stopped prior to the gel point to obtain soluble polymers. The location of the complementary functional groups A and B on different molecules allows the alteration of the monomer composition in the feed and, consequential, the ratio of unreacted groups of both types in the final polymer.

Usually, hyperbranched polymerizations yield very heterogeneous products. Besides an extremely broad molecular weight distribution, the different structural units can vary in their content and sequence within the polymer branches. The characteristic structural units of hyperbranched polymers were named as terminal (t), linear (l), and dendritic (d). Their relative content defines the degree of branching (DB) and, in connection with their sequence, the shape and the radius of gyration of the macromolecules. Side reactions like intramolecular cyclization and the reaction of two equal functional groups with each other can further complicate the situation. For kinetically controlled step-growth polymerizations, including $A_2 + B_3$ systems, a high tendency to form multiple cycles per molecule is well documented.[14] A control of the structure necessities thus an understanding of the structure development during the hyperbranched polymerization. This leads to a great interest in theories which are able to explain and predict the development of the structural units in the course of polymerization. The two main approaches to polycondensation are a statistic one, mostly based on Monte Carlo simulations, and a kinetic or thermodynamic one, that relies on fundamental equations describing the system and properties of the system.[15] The first approaches to branched polymerizations came from the theory of gelation and were developed by Flory[13] and Stockmayer.[16] A further deepening of the theories describing the reaction of AB_x type monomers has emerged with the growing interest in hyperbranched polymers during the 1990s. Möller et al.[17] and Müller et al.,[18] respectively, described the conversion dependence of the structural units during polycondensation and SCVP of AB_2 monomers. The degree of branching as introduced by Frechet and Hawker[6] and Kim[5] was redefined by Frey et al.[19] based on the growth directions to better suit the products at low conversion. In contrast to Frechet's equation, the calculation is only based on the relative concentrations of dendritic (d) and linear (l) units (eq 1). Furthermore, Frey et al. enlarged the discussion to AB_3 type monomers and the simulation of new techniques as core dilution/slow monomer addition.[19] Kinetic studies of branched polymerizations were carried out, e.g., by Hult et al.,[20] Galina et al.,[21] McCoy,[22] and Schmaljohann et al.[23,24] The latter analyzed a nonideal hyperbranched polymerization[24] based on a kinetic model that allows the calculation of the concentrations of the structural units also for different reaction rate constants for each primary reaction.[25]

* To whom correspondence should be addressed: Fax ++49 351 4658 565; e-mail komber@ipfdd.de.

† Present address: Institut Charles Sadron CNRS, 6 rue Boussingault, 67083 Strasbourg Cedex, France; e-mail reisch@ics.u-strasbg.fr.

‡ E-mail: voit@ipfdd.de.

10.1021/ma070812g CCC: $37.00
Published on Web 08/21/2007

$$DB_{Frey} = \frac{2d}{2d + l} \quad (1)$$

The structure formation and the theory of $A_2 + B_3$ systems were mainly studied in the context of gelation thus focusing on prediction of the gel point, molar masses, and the ratio of sol and gel fraction.[14] Theories describing in detail the development of the system before the gel point have been proposed by Dusek et al.,[26] Long et al.,[27] and Schmaljohann and Voit.[28] Dusek et al. described the influence of the composition and the relative reactivities on the critical molar ratio at which no gelation takes place as well as the accompanying development of molar mass and molar mass distribution.[26] Long et al. studied theoretically and experimentally the development of the molar masses and the DB with conversion.[27]

Schmaljohann and Voit developed a kinetic model similar to the one applied to the analysis of AB_2 polymerizations[24,25] that allows the description of the content of structural units in an $A_2 + B_3$ system for different kinetic situations.[28] The application of this theoretical approach in the analysis and interpretation of experimentally determined structural compositions of hyperbranched $A_2 + B_3$ polymers depending on monomer conversion is the topic of the presented article. Two combinations of different A_2 and B_3 monomers were studied at different monomer ratios. Additionally, for one system the effects of successive addition of the monomer feed were investigated.

The two systems chosen for the kinetics are based on 1,1,1-tris(4-hydroxyphenyl)ethane (THPE, Figure 1) and its silylated derivative 1,1,1-tris(4-trimethylsiloxyphenyl)ethane (TMS−THPE) for the B_3 monomer because of the accessibility of the structural subunits by ^{1}H NMR spectroscopy. Furthermore, lower conformational flexibility compared with aliphatic systems combined with spatial well-separated B functionalities should suppress at least the formation of small cycles. Best control of the reaction was obtained by the combination of TMS−THPE as the B_3 monomer and terephthaloyl chloride (TCl) as the A_2 component. In the second system, composed of THPE and adipic acid (AA), side reactions due to the high reaction temperature could not be prevented. Nevertheless, it was studied because of the separation of the two A functional groups by four methylene groups in AA should lead to an independent reactivity of both carboxylic groups. The kinetics of these systems were studied using ^{1}H NMR spectroscopy to determine the monomer conversion and the content of structural units. The experimental results were fitted with the kinetic model and the obtained kinetic parameters were discussed based on chemical principles.

Theoretical Background

The kinetic model of Schmaljohann and Voit[28] giving the theoretical background of this study is based on the possible reactions in the system that lead to the formation of the hyperbranched polymers. The reaction pathways, the different structural units present in the system as well as their nomenclature used throughout this article are summarized in Figure 2.[29] Capital letters stand for nonreacted functional groups, lower case letters stand for reacted ones. The rate constants k((A)(B)) are the rate constants for the reaction of one A group of the structural unit (A), i. e. A_2 or Aa, with one B group of the structural unit (B), i. e. B_3, B_2b or Bb_2. The rate constants discussed herein are relative rate constants with the value of $k(A_2B_3)$ for the reaction of a A functional group in the A_2 monomer with a B functional group in the B_3 monomer being fixed to 1 (compare also with the Supporting Information).

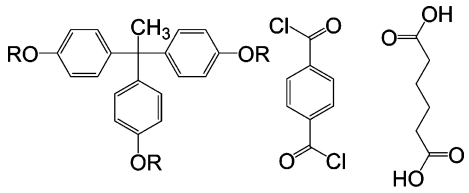

R = H: THPE TCl AA
R = Si(CH$_3$)$_3$: TMS-THPE

Figure 1. Formulas of the A_2 and B_3 monomers.

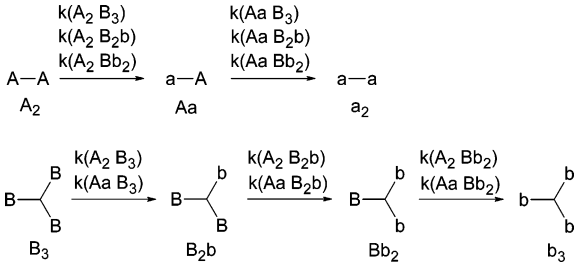

Figure 2. Reaction pathways and notation of the structural units and the reaction rate constants of an $A_2 + B_3$ system.

$$K = \begin{bmatrix} k(A_2B_3) & k(A_2B_2b) & k(A_2Bb_2) \\ k(aAB_3) & k(aAB_2b) & k(aABb_2) \end{bmatrix}$$

Figure 3. General matrix of the rate constants for a $A_2 + B_3$ system.

Table 1. Changes of the Structural Units along One Row or Column and Relation to the K Matrix of Reaction Rate Constants (Figure 2)

$A_2 + B_3$, k(A_2 B_3)	$A_2 + B_2b$, k(A_2 B_2b)	$A_2 + Bb_2$, k(A_2 Bb_2)	⇒	$A_2 \rightarrow Aa$
$Aa + B_3$, k(Aa B_3)	$Aa + B_2b$, k(Aa B_2b)	$Aa + Bb_2$, k(Aa Bb_2)	⇒	$Aa \rightarrow a_2$
⇓	⇓	⇓		
$B_3 \rightarrow B_2b$	$B_2b \rightarrow Bb_2$	$Bb_2 \rightarrow b_3$		

As explained in refs 25 and 28, it is useful to summarize all possible reactions and their rate constants in a matrix notation. The matrix of the six rate constants is given in Figure 3 . The columns correspond to reactions where a B group in one particular structural unit reacts with an A group in one of the A containing units, and the rows correspond to reactions of an A group in one of the two A containing units with a B group in different units (compare Table 1). The concentration of the different structural units as a function of conversion can be obtained from the iterative integration of a system of differential equations.

In the polymerization of an $A_2 + B_3$ system, there are several general kinetic situations possible depending on the influences of the reaction of one or two functional groups on the reactivity of the remaining functional groups. If there is no influence of the reaction of functional groups on the reactivities of the remaining ones, that is the rate constants for all functional groups in all structural units are equal and the functional groups react entirely independently, then the system can be described by the unity matrix for the relative rate constants (**K**(1), Table 2). To illustrate retardation and acceleration effects on the **K** matrix, Table 2 gives four examples for the arbitrary case that retardation/acceleration decreases/increases the rate constant by a factor of 2 per reaction of one functional group in the molecule. If the reaction of one B site leads to a retardation of the subsequent reactions, the corresponding matrix has the form of the matrix **K**(2) whereas acceleration results in **K**(3). In both cases, it was supposed that the reaction of one A group has no effect on the reactivity of the other one. In the case of the A groups, the matrix takes the form **K**(4) for a retardation and

Table 2. Matrices Describing the Cases of Same Reaction Rates (K(1)) and Retardation or Acceleration of the Rate Constants by Arbitrary Factors of 0.5 and 2, Respectively, Due to Reaction of a B Group (K(2) vs K(3)) or an A Group (K(4) vs K(5))

$$K(1)=\begin{bmatrix}1 & 1 & 1\\ 1 & 1 & 1\end{bmatrix}$$

$$K(2)=\begin{bmatrix}1 & 0.5 & 0.25\\ 1 & 0.5 & 0.25\end{bmatrix} \qquad K(3)=\begin{bmatrix}1 & 2 & 4\\ 1 & 2 & 4\end{bmatrix}$$

$$K(4)=\begin{bmatrix}1 & 1 & 1\\ 0.5 & 0.5 & 0.5\end{bmatrix} \qquad K(5)=\begin{bmatrix}1 & 1 & 1\\ 2 & 2 & 2\end{bmatrix}$$

the form **K**(5) for an acceleration due to reaction of the first A group. Influences of the reactions of both A and B groups on the reactivities might also be possible, resulting in a combination of the matrices, i.e., in more complex relations between the different relative rate constants.

In order to allow the comparison of the experimental results with the model, the system has to fulfill a number of requirements. First of all the relative concentrations of the different structural units have to be accessible as they represent the input data for the comparison with the model. This is usually accomplished by NMR spectroscopy but requires that all reaction products are soluble in solvents appropriate for NMR measurements and that it is possible to distinguish and to quantify the structural units in the spectrum. Furthermore, reactions have to take place in a homogeneous phase because the model does not account for, e.g., diffusion effects typical for heterogeneous systems or effects of interfaces. The overall concentration of reacted and nonreacted functional groups of both types should be constant during the whole course of the reaction; i.e., neither the monomers nor oligomers should escape from the reaction mixture. Excessive side reactions as well as cyclization would also lead to problems when comparing the experiments with theory. Intramolecular cyclization reactions are monomolecular and their rates depend on rate constants k_{intra} and on the concentration $[M_i]$ of the cycle-forming molecule M_i. The intermolecular reactions of M_i with rate constants k_{inter} are assumed to be bimolecular in our case and their rates depend on both $[M_i]$ and the concentration of the reaction partner for a certain pathway. Whereas k_{intra} and k_{inter} depend on the size and shape of M_i the concentrations of the different species M_i vary with conversion. Effectively, the total reaction order of the system changes with conversion. The total reaction rate for M_i or a subunit is that of a complex system where extensive polymerization competes with macrocyclization which cannot be separated in our approach. Values for the ratio k_{intra}/k_{inter} between 0.03 mol/L for 20-membered rings to ~0.005 mol/L for larger than 100-membered rings are reported as realistic values for the reaction of AB monomers.[30] High concentrations as applied by us enhance bimolecular intermolecular reactions. Thus, we assume that the contribution of intramolecular reactions which definitely occur in our systems is within the error of the method applied. The prove of such reactions can occur by MALDI−TOF measurements[14,31] and their effect on the polydispersity of the products can be significant,[14,26,27,32,33] but both aspects were outside the scope of this study.

Experimental Section

Materials. Adipic acid (AA, ≥ 99.0%) and chlorotrimethylsilane (≥99.0%) were purchased from Merck, hexamethyldisilazane (HMDS, > 98%), terephthaloyl chloride (TCl, ≥ 99.0%), and triethylamine hydrochloride (≥99.0%) were purchased from Fluka, and 1,1,1-tris(4-hydroxyphenyl)ethane (THPE, ≥ 99.0%), toluene (p.a.), and and 4-ethylphenol (≥99.0%) were purchased from Aldrich.

Synthesis of 1,1,1-Tris(4-trimethylsiloxyphenyl)ethane (TMS—THPE). THPE (15.318 g, 50 mmol), hexamethyldisilazane (24.209 g, 150 mmol), and chlorotrimethylsilane (16.296 g, 150 mmol) were refluxed for 16 h in 200 mL of toluene. After rotoevaporation of the solvent, a white powder was obtained. The crude product (98% yield) was further purified by distillation over a short-path apparatus (10^{-2} mbar, 200 °C) under an argon atmosphere resulting in 15 g of a white crystalline product (60% yield). Mp = 120 °C. ^{1}H NMR ($CDCl_3$): δ = 0.25 (s, 27H, Si−CH_3), 2.09 (s, 3H, C−CH_3), 6.91 (d, 6H, H_{ar} *meta* to −OTMS), 6.71 (d, 6H, H_{ar} *ortho* to −OTMS).

Synthesis of (4-Ethylphenoxy)trimethylsilane. A 10 g sample of 4-ethylphenol (82 mmol) was put into a two-necked flask with reflux condenser and 20 g (124 mmol) of hexamethyldisilazane was added. After addition of 120 mL of toluene, the clear solution was refluxed for 12 h. The major part of the solvent was removed by rotoevaporation. The product was purified by distillation at 146 °C and 115 mbar under an argon atmosphere. (4-Ethylphenoxy)-trimethylsilane was obtained as a clear liquid in a yield of 75%. ^{1}H NMR ($CDCl_3$): δ = 0.26 (s, 9H, Si−CH_3), 1.22 (t, 3H, CH_3), 2.59 (q, 2H, CH_2), 7.06 (d, 2H, H_{ar} *meta* to −OTMS), 6.76 (d, 2H, H_{ar} *ortho* to −OTMS).

Polymerization of TCl/TMS—THPE. TMS−THPE (10.0 g, 19.13 mmol) and terephtaloyl chloride (5.82 g (28.67 mmol), 3.88 g (19.11 mmol), and 2.91 g (14.33 mmol), respectively, corresponding to the A_2:B_3 ratios of 3:2; 1:1 and 3:4) were thoroughly mixed and placed under argon in a dry three-necked flask equipped with argon inlet, condenser and magnetic stirring bar. The reaction flask was put in an oil bath preheated at 145 °C, and a weak argon flow was adjusted. When a homogeneous melt has been obtained, the catalyst, triethylamine hydrochloride (0.5 mol % relative to TMS−THPE, i.e., 0.013 g; 0.01 mmol), was added. Samples were taken out of the reaction mixture at certain times; for this the inert gas stream and the stirring were interrupted. The samples were immediately placed in NMR tubes with 0.7 mL of DMSO-d_6 and one drop of D_2O to hydrolyze the acid chloride and TMS groups. Slight heating was sometimes necessary to dissolve the samples. A conversion of 69% of the A groups was reached after 218 min in the case of an A_2:B_3 ratio of 3:2, after 175 min for 1:1, and after 142 min for 3:4.

Polymerization of TCl/TMS—THPE with Addition of Monomer Mixture. The polymerization was performed as described above, but only 2.5 g (4.78 mmol) of TMS−THPE and 1.46 g (7.19 mmol) of terephthaloyl chloride were employed (A_2:B_3 = 3:2). The conversion of the functional groups was followed by immediate NMR measurements on the samples taken. At a conversion of about 57%, the same amount of a 3:2 mixture of both monomers as employed in the beginning (2.5 g of TMS−THPE and 1.46 g of TCl, reduced by the quantity taken out until that point as NMR samples) was added. Argon gas stream and stirring were stopped for about 5 min in order to minimize the loss of terephthaloyl chloride by evaporation. The system with a conversion of 57% is mixed with a system having a conversion of 0% by addition of fresh monomer feed. This leads to a decrease of the measured overall conversion immediately after monomer feed addition to about 27% as determined by NMR. This procedure was repeated two more times; when the system had again reached a conversion of 57% the second addition of monomer mixture decreased the overall conversion to 35%, and the third addition was performed when a conversion of 55% was reached after the second addition. However, after the third addition, the system became inhomogeneous and the kinetic was stopped.

Polymerization of AA/THPE. THPE (10 g, 33 mmol) and adipic acid (7.17 g, 49 mmol) were thoroughly mixed and placed under argon in a dry three-necked flask equipped with argon inlet, condenser, and magnetic stirring bar. The reaction flask was put in an oil bath preheated at 185 °C and constantly let under a slight argon flow. The reaction mixture melted within 5 min even though a small part of the mixture remained initially unmelted on the wall of the flask. Two drops of dibutyltin diacetate were added to the melt. About 7 h after the addition of the catalyst, a completely homogeneous and transparent melt was obtained, and the part

initially unmelted had melted. The reaction was performed during 90 h and catalyst was added several times after the conversion has reached 50%. Samples were continuously taken out of the reaction mixture and immediately dissolved in DMSO-d_6.

Reaction of (4-Ethoxyphenoxy)trimethylsilane with TCl. (4-Ethylphenoxy)trimethylsilane (5.00 g, 28 mmol) and terephthaloyl chloride (6.41 g, 32 mmol) were weighed under argon in a dry three-necked flask equipped with argon inlet, condenser, and magnetic stirring bar. The reaction flask was put in an oil-bath preheated at 145 °C and a slight argon flow was adjusted. A turbid melt was obtained that became clear shortly after the addition of the catalyst (10 mg of triethylamine hydrochloride). The reaction was carried out during 5 h. Several samples were taken out of the reaction mixture; for this the inert gas stream and the stirring were interrupted. The samples were immediately placed in NMR tubes with 0.7 mL of DMSO-d_6 and one drop of D_2O to hydrolyze acid chloride and TMS groups.

NMR Measurements. The NMR spectra were obtained on a Bruker DRX 500 spectrometer operating at 500.13 MHz for ^{1}H and 125.77 MHz for ^{13}C. Solutions in DMSO-d_6 (lock and internal standard, $\delta(^1H) = 2.50$ ppm, $\delta(^{13}C) = 39.6$ ppm) were measured at 303 K. The ^{13}C spectra were obtained using inverse gated decoupling, $\pi/2$ ^{13}C pulses and a pulse delay of 12 s. ^{1}H−^{1}H and ^{1}H−^{13}C shift correlated spectra were recorded using the standard pulse sequences provided by Bruker. The error in determining the mole fractions of the different units from the integral values is estimated to be ≤1.5 mol % from repeated integrations and deconvolutions, respectively.

Simulations. Simulation of the kinetic curves has been carried out by calculation of the differential equations using an iterative process. Each step is normalized to the conversion p and counts $0.001p$ giving between 680 and 950 steps of iteration depending on the experimentally reached maximal conversion, that is the conversion at the experimental gel point (p_c). Here, we followed the procedure described in more detail in refs 24, 25, and 28. The relative concentrations of the structural units and the degree of branching were calculated as a function of the conversion of A groups (p_A) from $p_A = 0$ up to $p_{c,A}$, the conversion of A groups at the experimentally observed gel point. The calculation of the degree of branching is based on eq 1 with Bb_2 representing the l (linear) units and b_3 representing the d (dendritic) units:

$$DB_{Frey} = \frac{2[b_3]}{2[b_3] + [Bb_2]} \quad (2)$$

The simulation of the kinetic graphs for the stepwise addition of monomer mixture has been carried out in a way that the value of monomer conversion p_A at the moment of monomer feed addition was taken from the experimental value determined for the sample taken immediately before addition. This approximation is legitimate because of the low reaction rate. For the simulations with loss of A_2 monomer a constant loss of A_2 up to a conversion of A groups of 30% was used. The concentrations were normalized to the calculated concentration of all structural units present.

Results and Discussions

(a) Polymerization of A_2 Monomer TCl and B_3 Monomer TMS—THPE. The catalyzed reaction of a phenoxysilane with an acid chloride (Figure 4) is a well-known reaction for polyester formation frequently used for the synthesis of hyperbranched polymers. The possibility of purifying the monomers by distillation, no reaction of the two functional groups even at temperature well above 100 °C unless a catalyst is added and the absence of side reactions during the polymerization are favorable for the use of this reaction for the kinetics.

Three different ratios of A_2 to B_3 monomer were studied for this system: the 3:2 ratio with equal concentration of the functional groups, the 1:1 ratio with an excess of B functionalities and the 3:4 ratio having a 1:2 ratio of the functional

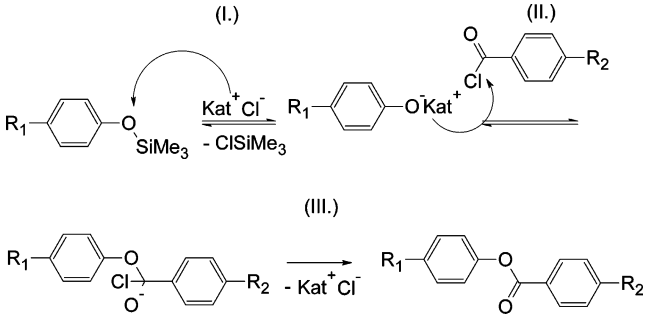

Figure 4. Mechanism of the reaction of a phenoxysilane with an acid chloride as proposed by Kricheldorf and Schwarz.[33]

groups A and B as for an AB_2 system. The theoretical gel points for the 3:2 and 1:1 ratios can be calculated to 70.7% and 86.6% conversion of A functionalities, respectively, whereas for the 3:4 ratio no gelation should occur before complete conversion of A groups.[28] Furthermore, the stepwise addition of a $A_2 + B_3$ monomer mixture to a 3:2 monomer ratio was studied.

The quantification of structural units in dependence on the reaction progress is based on the interpretation of ^{1}H NMR spectra. It has been found to be more convenient to completely hydrolyze the unreacted acid chloride and silanoxy groups in the polymeric product prior to the NMR analysis as those tend to hydrolyze partially due to the water content usually present in DMSO-d_6. This was achieved by deliberately adding a small amount of D_2O to the DMSO-d_6. Therefore, the polymers investigated by NMR spectroscopy contained acid and phenol groups as functionalities.

By combined analysis of ^{1}H, ^{13}C, ^{1}H−^{1}H shift correlated (COSY), and ^{1}H−^{13}C one- and multiple-bond shift correlated (HMQC, HMBC) spectra, a comprehensive ^{1}H and ^{13}C signal assignment was achieved (see Supporting Information). We do not describe this analysis in detail but discuss some results with respect to the quantitative structural analysis. Fortunately, it was possible to identify well separated ^{1}H signals corresponding to the B_3 monomer and the B_2b, Bb_2, and b_3 units and also to the different structural units obtained from terephthaloyl dichloride (A_2 monomer, Aa and a_2 units) in the product spectra (Figure 5b). The relative contents of B_3 and its reaction products have been calculated from the signal intensities of their methyl group signals (H^1). The aromatic protons H^9 and $H^{9'}$ show typical singlets for the symmetrically substituted units A_2 and a_2, respectively, and two doublets for Aa. An additional fine structure observed for $H^{9'}$, $H^{4'}$, and $H^{5'}$ is attributed to the nature of the unit linked to the reacted functional groups a and b (B_2b, Bb_2 or b_3; Aa or a_2). A quantification of those diads was not possible due to signal overlap.

Before discussing the results of polymer kinetics two experimental sources of error should be considered: loss of monomers from the reaction mixture and hydrolysis of functional groups.

Monomer systems of the $A_2 + B_3$ type have the advantage that one can alter the composition of the polymer by employing different ratios of A_2 to B_3 monomer. On the other hand the volatility of one or both of the monomers can lead to a change of the overall composition of the system during the course of the polymerization. This causes problems when studying the kinetics of such systems as not only the starting composition and the reactivity of the functional groups in the different structural units but also the kinetics and the extent of the volatilization can influence the products obtained.

The development of the ratio of all units derived from A_2 to all units derived from B_3 (ratio A_2:B_3) is represented in Figure

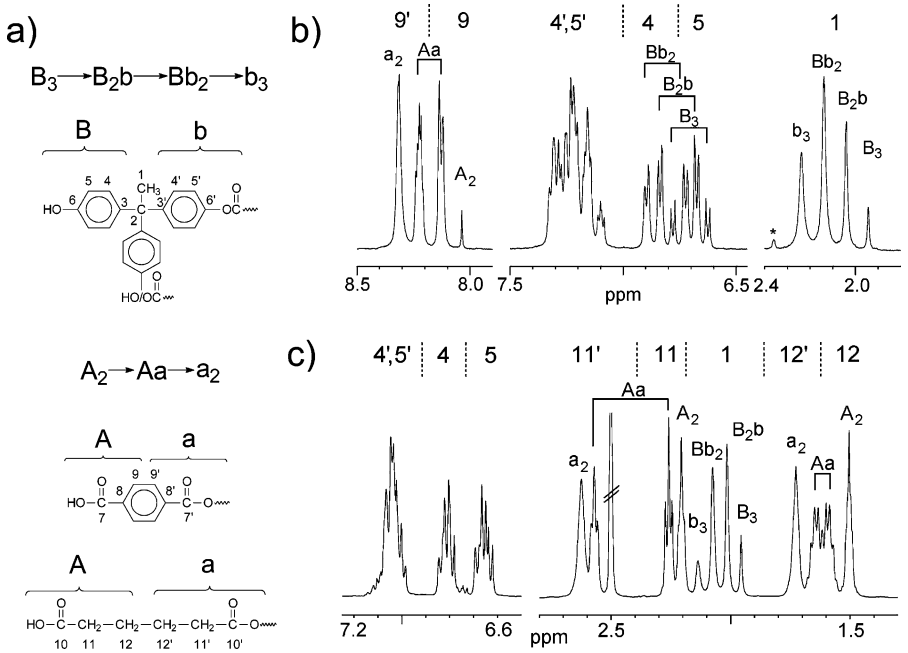

Figure 5. Numbering of the atom positions for the unreacted (A, B) and reacted (a, b) parts of the different substructures (a) and 500 MHz ^{1}H NMR spectra of a hydrolyzed TCl/TMS−THPE copolymer (A_2:B_3 = 3:2; $p_A = p_B = 0.66$) (b) and of an AA/THPE copolymer (A_2:B_3 = 3:2; $p_A = p_B = 0.51$) (c) in DMSO-d_6 with signal assignments to the different structural units (∗, ^{13}C satellite of DMSO-d_6).

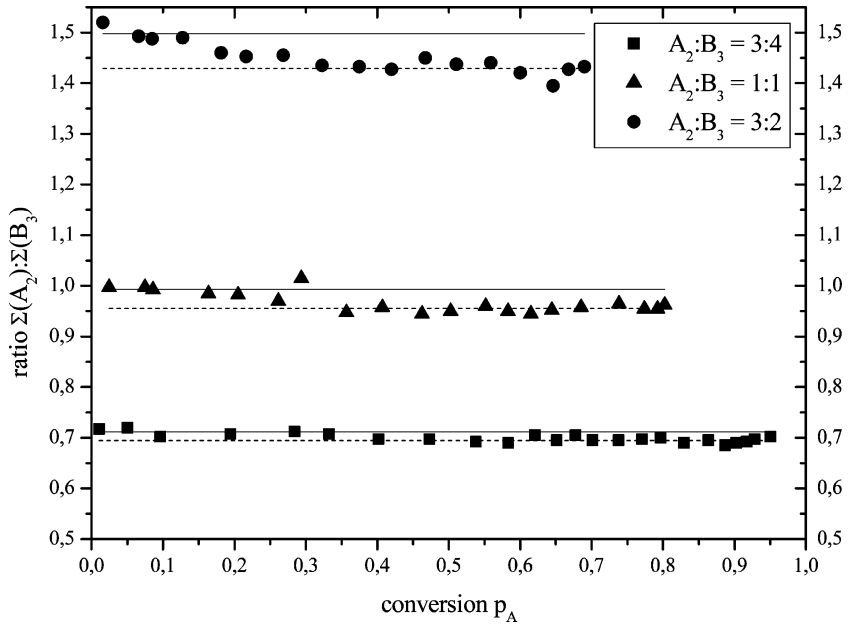

Figure 6. Development of the ratios of the sum over all structural units derived from A_2 ($\Sigma(A_2)$) to the sum over all structural units derived from B_3 ($\Sigma(B_3)$) as a function of the conversion of the A groups (p_A) for the system TCl/TMS−THPE and different starting ratios A_2:B_3. The points stand for the experimental values, the full lines correspond to the mean values of the first four experimental points, and the dashed lines correspond to the mean values of the last 10 experimental points.

6 for the three different kinetics. One observes a slight decrease of this ratio up to a conversion of about 25−30% after which a plateau value is reached. This corresponds to a relative loss of the overall concentration of units derived from A_2, indicating that terephthaloyl chloride (A_2 monomer) is subject to volatilization at the conditions used for the polymerization. The relative loss of A_2 up to the plateau value depends on the starting ratio and is about 4.7% for A_2:B_3 = 3:2, 4.4% for A_2:B_3 = 1:1, and 3.5% for A_2:B_3 = 3:4, respectively.

We suppose that the evolving gaseous chlorotrimethylsilane is predominantly responsible for taking the terephthaloyl chloride out of the reaction mixture especially in the initial phase of the reaction. This effect levels off with increasing conversion as the concentration of A_2 monomer decreases and increasing viscosity of the reaction mixture and a decreasing reaction rate slow down the liberation of chlorotrimethylsilane. The rate of volatilization and thus the loss of A_2 monomer is higher for higher starting concentrations of A_2, i. e. for a more vigorous reaction in the beginning.

To be able to compare the experimental results with the simulation the nature and extent of possible side reactions that alter concentrations of structural units or reactivity of functional

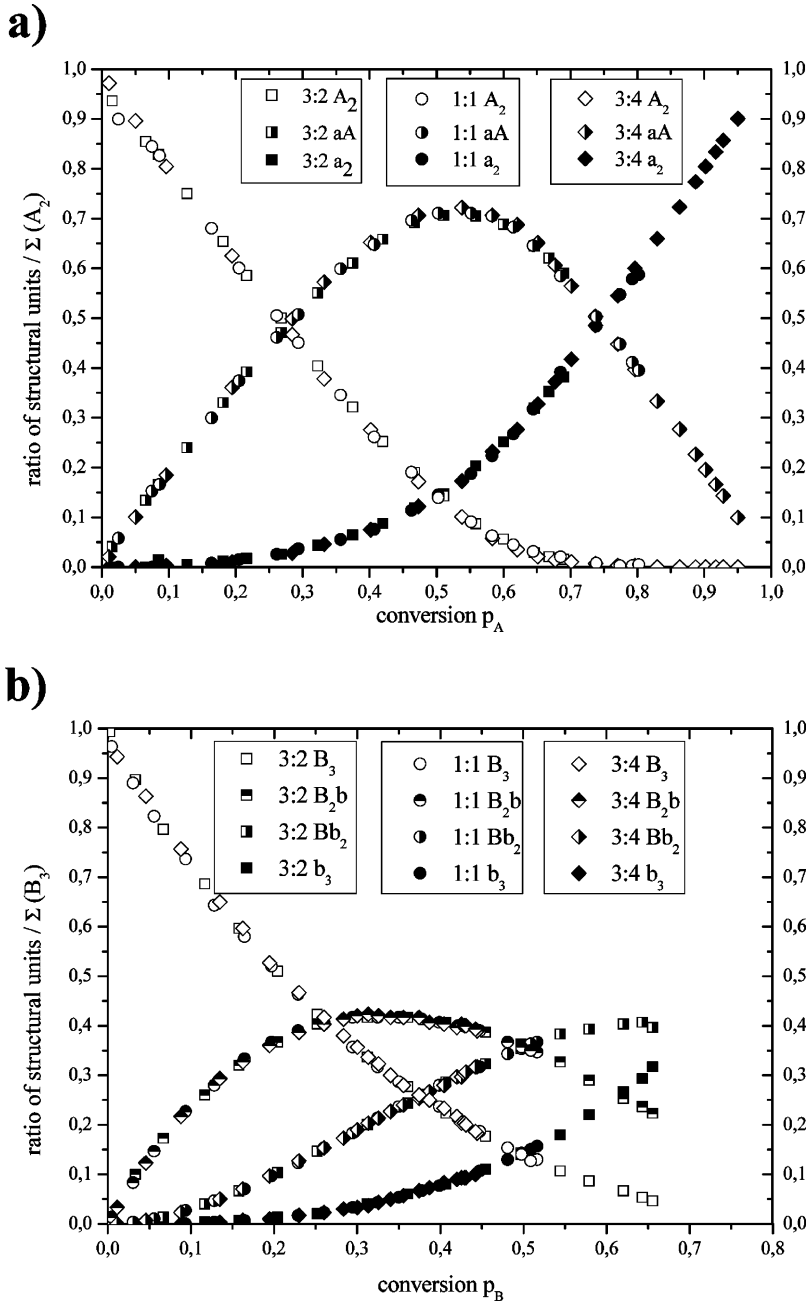

Figure 7. Conversion dependence of the structural units (a) A_2, Aa, and a_2 as a function of p_A and (b) B_3, B_2b, Bb_2, and b_3 as a function of p_B for the polycondensation of TCl (A_2) with TMS−THPE (B_3) where the ratios of A_2 to B_3 in the beginning were 3:2, 1:1 and 3:4 (NMR data are normalized to the sum of all units derived from (a) A_2 or (b) B_3, respectively).

groups should be known. For the system discussed here no side products are detected. The only possible side reaction is thus the hydrolysis of the functional groups as both siloxy ethers and acid chlorides are moisture sensitive. However, since, e.g., in the case of the A_2:B_3 ratio 3:4 about 96% of the A groups have reacted at the gel point and the ^{1}H signal of the A_2 monomer disappears completely and since the concentration of reacted A and B groups is equal, we concluded that there is no or only very little hydrolysis of the acid chloride and even less of the more hydrolysis stable siloxy ethers during the reaction.

Development of the Structural Units and of the Degree of Branching with Conversion for the System TCl/TMS—THPE and Its Simulation by Relative Rate Constants. We have analyzed the experimental determined contents of subunits up to the gel point, i.e., the last point in the figures corresponds to the last sample that was entirely soluble.

A plot of the relative concentrations of the units derived from the A_2 monomer, normalized to the sum of A_2, Aa, and a_2 units, as a function of p_A, shows that the curves for the different ratios are superimposed (Figure 7a). The same is true for the B_3, B_2b, Bb_2 and b_3 units when they are plotted as a function of p_B (Figure 7b). This is a first indication that the kinetics shows, if at all, a very small dependence on the monomer ratio.

This can also be concluded from a plot of the degree of branching according to Frey (eq 2) as a function of p_B (Figure 8a). The development of the DB as a function of p_B is virtually identical for all three ratios employed. The ratio determines the structure of the products over the conversion that can be reached before gelation and thus influences the DB obtained. This means

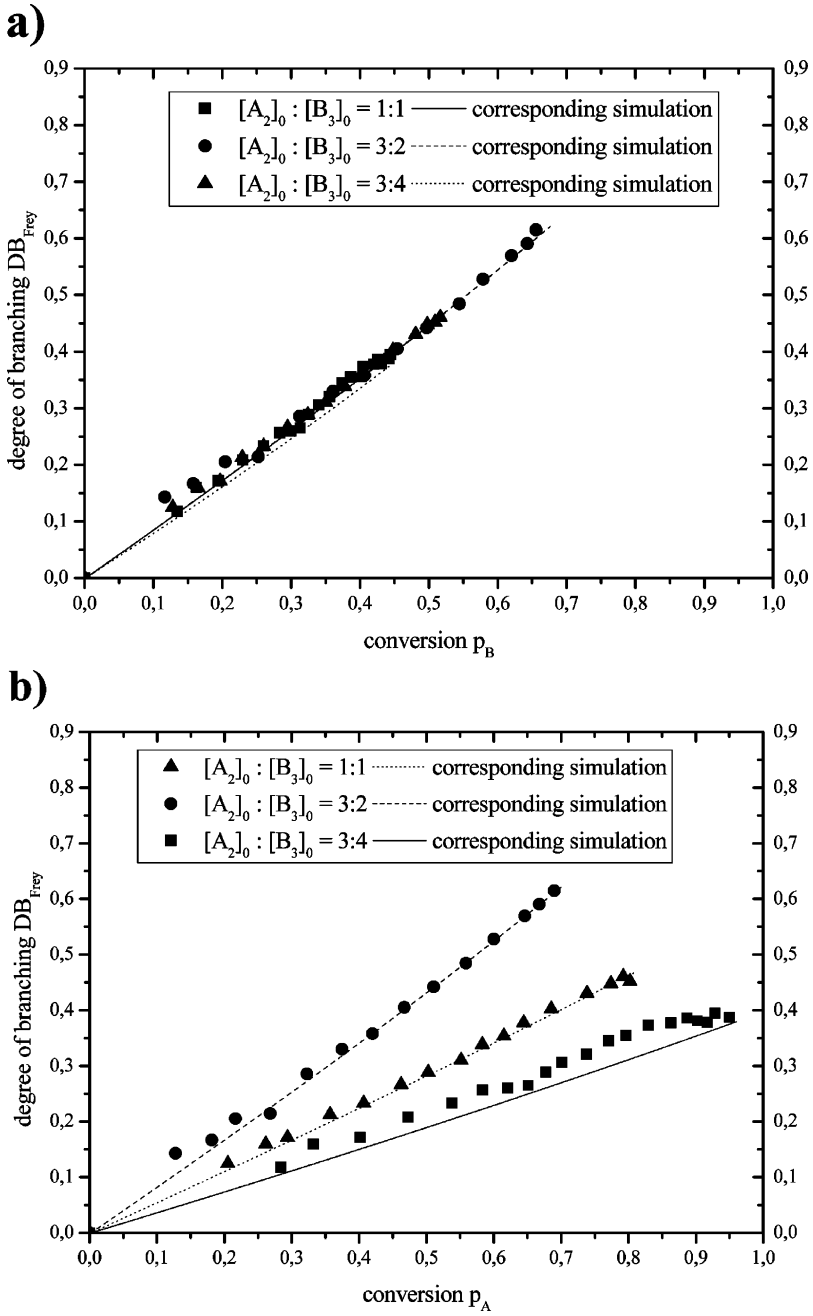

Figure 8. Development of the degree of branching DB_{Frey} with conversion (a) of the A groups and (b) of the B groups in the system TCl/TMS−THPE. The symbols give the experimental data points, the lines stand for fits obtained with the calculated relative rate constants for this system.

that for soluble polymers the maximum achievable DB as defined here depends only on the conversion of the B groups at the gel point. Naturally, this critical conversion is determined by the initial A_2 to B_3 ratio. DB as a function of p_A is shown in Figure 8b. Both plots are related by eq 3 which gives the relation between p_B and p_A:

$$p_A = rp_B \tag{3}$$

where r is the ratio of all B to all A groups in the system (r = 1, 1.5, and 2 for A_2:B_3 = 3:2, 1:1 and 3:4, respectively). A stretching of the x-axis results for $r > 1$.

It should be noted that the degree of branching as calculated here from the content of linear (Bb_2) and dendritic (b_3) units provides no information on the long range structure of the macromolecules obtained. In fact a high degree of branching states that the former B_3 units are highly reacted with A_2 but there is no information whether also the second A unit of the bonded A_2 monomer has reacted or not.

In order to facilitate the comparison of the different experiments, the obtained concentrations for the structural units are normalized in a way that the overall concentration of all structural units, i.e., those derived from the A_2 as well as those derived from the B_3 monomer, equals 1 (see Supporting Information and Figures 9 and 10).

Figures 9 and 10 compare the experimental data points with the curves calculated for an equal and independent reactivity of all functional groups (dotted lines), represented by the **K**(1) matrix (Table 2). It is obvious for the A_2, Aa, and a_2 units (Figure 9) that the **K**(1) matrix does not properly describe the reaction. In the case of the different B units (Figure 10), the deviations between both calculated curves and experimental data are less expressed but also here the deviations are obvious. The content of a_2 units is lower than expected for all p_A values

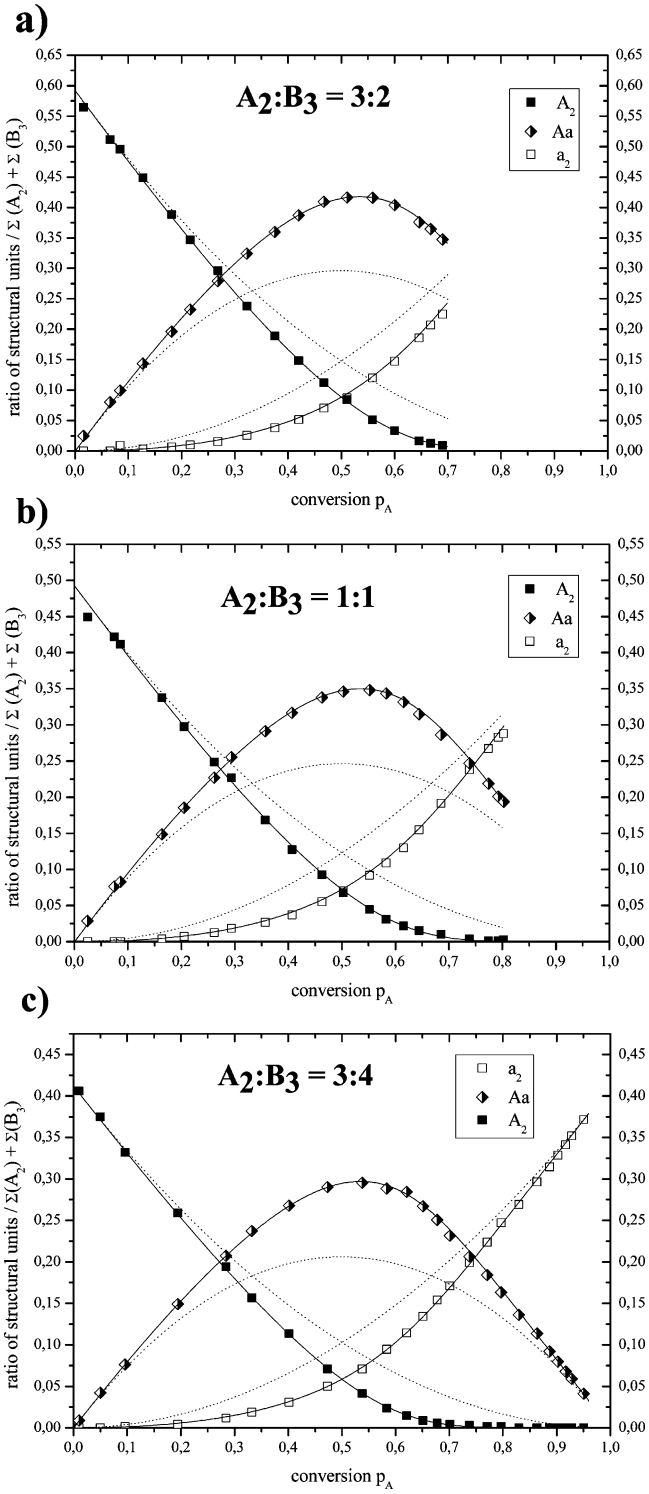

Figure 9. Comparison of experimental data and simulation for the A_2, Aa and a_2 units in the system TCl/TMS−THPE for an initial ratio of A_2:B_3 of (a) 3:2, (b) 1:1, and (c) 3:4. The symbols give the experimental data for the structural units as a function of conversion p_A, the lines give the data obtained from a simulation with the fitted matrix, the dotted lines give the data from a simulation for equal and independent reactivity of all functional groups (**K**(1) matrix, ideal case). All data are normalized to the sum of all structural units.

allowing the qualitative conclusion that reaction of the first A site results in retardation of the second condensation step.

By contrast, the content of b_3 units is slightly increased indicating an acceleration of the reactions of the B sites after the reaction of one or two B sites in the unit.

To obtain a quantitative picture, the experimental data for the units derived from A_2 and B_3 monomer, respectively, were fitted separately varying the rate constants in the rows (columns) but keeping constant the ratio within the columns (rows). The resulting K matrices were then combined to give the final K matrices for the different A_2:B_3 ratios. This procedure is based on the assumption, that the relative change of reactivity with regard to one A(B) function, depends only on the state of the other A(B) functions in the $A_x a_y$ ($B_u b_v$) unit and not on the type of unit of the B(A) function it reacts with. One specific relative rate constant (e.g., k(Aa B_2b)) for the reaction of an A function (in Aa) with a B function (in B_2b) is then the product of the two relative reactivities (that is A in Aa and B in B_2b). It is

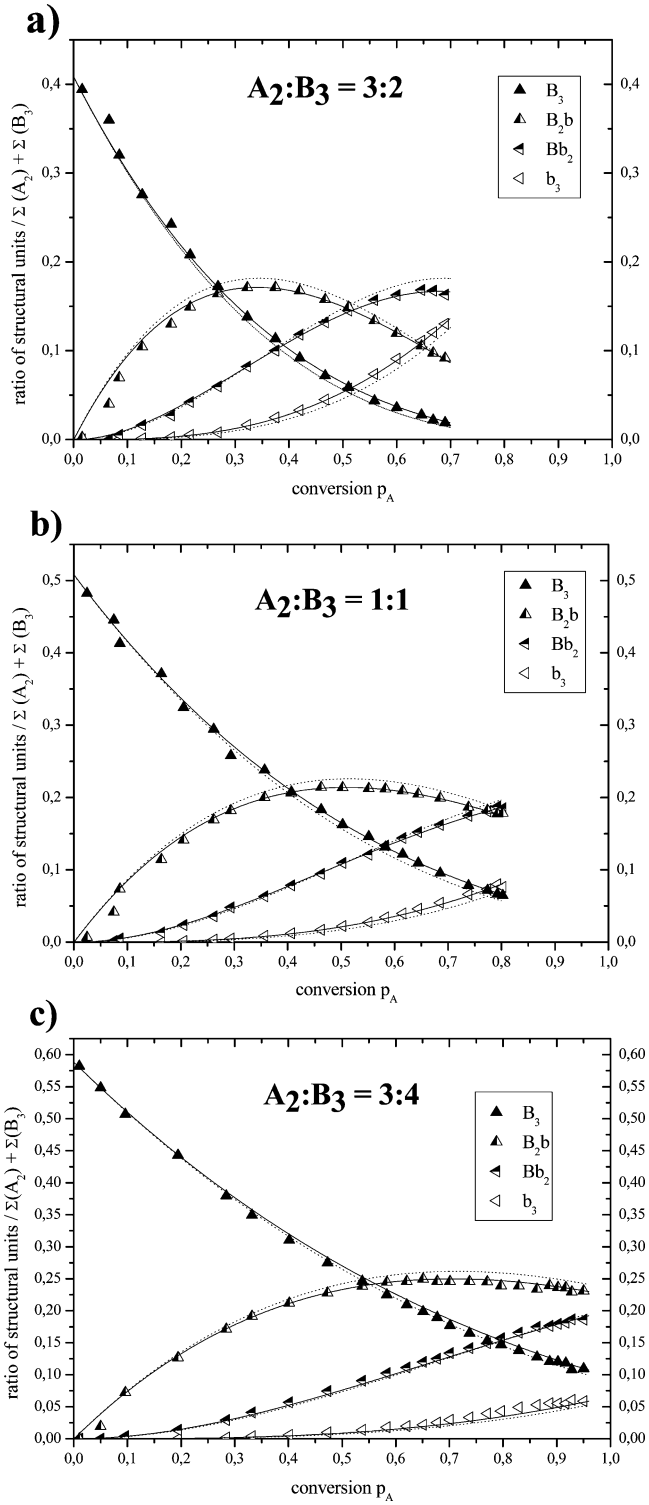

Figure 10. Comparison of experimental data and simulation for the B_3, B_2b, Bb_2 and b_3 units in the system TCl/TMS−THPE for an initial ratio of A_2:B_3 of (a) 3:2, (b) 1:1, and (c) 3:4. The symbols give the experimental data as a function of conversion p_A, the lines give the data obtained from a simulation with the fitted matrix, and the dotted lines give the data from a simulation for equal and independent reactivity of all functional groups (**K**(1) matrix, ideal case). All data are normalized to the sum of all structural units.

obvious from Figures 9 and 10 that these matrices yield a very good agreement between simulation (full lines) and experiment.

The optimized K matrices for the three different A_2:B_3 ratios are given in Table 3. There should be no effect of the A_2:B_3 ratio on the k values and in fact all three simulations result in very similar K matrices. The small deviations can be explained both by experimental influences, i.e., different viscosities of the reaction mixtures, and by the fitting procedure. The fitting is performed with respect to the absolute differences between simulated and experimental data. Very small absolute differences between experimental data and simulation, i.e., for b_3 units at

Table 3. Relative Rate Constants Matrices Resulting from the Fitting Procedure for the System TCl/TMS−THPE with Initial Ratios of A_2:B_3 of (a) 3:2, (b) 1:1, and (c) 3:4

a)	b)	c)
$K_{3:2} = \begin{bmatrix} 1 & 1.14 & 1.28 \\ 0.32 & 0.36 & 0.41 \end{bmatrix}$	$K_{1:1} = \begin{bmatrix} 1 & 1.13 & 1.28 \\ 0.31 & 0.35 & 0.40 \end{bmatrix}$	$K_{3:4} = \begin{bmatrix} 1 & 1.11 & 1.18 \\ 0.29 & 0.32 & 0.34 \end{bmatrix}$

low concentrations, are underrepresented in the fitting process even if the relative differences are large. This results for the relative rate constants $k(A_2\ Bb_2)$ and $k(Aa\ Bb_2)$ (last column of the K matrix) which are associated with b_3 formation, in values that are too small and more subjected to errors. The effect is especially pronounced for fitting the data of the 3:4 system with the lowest b_3 content and hence the smallest absolute values. This furthermore leads to a lower agreement between simulation and experiment for the DB for the 3:4 ratio (Figure 8b).

In order to evaluate the influence of the loss of the A_2 monomer on the development of the structural units a standard simulation taking the mean value of the overall content of A_2, Aa and a_2 units as starting value was compared to a simulation in which the loss of the A_2 monomer was included in the simulation. It was found that the difference between the simulations was smaller than the experimental error. This justified the simulations without considering monomer loss as an additional variable.

Interpretation of the Observed Kinetic Situation. One observes a slight increase of the reactivity of the remaining B groups after the reaction of one or two B groups and a decrease of the reactivity of the second A group after reaction of the first one. A comparison of the relative changes for the reaction of one B unit from column 1 to 2 and 2 to 3 in the matrices in Table 3 shows that the acceleration is about 13% per B group reacted. The reactivity of the second A group decreases by about 70%. In order to explain these results a closer analysis of the different effects on the reactivity of the functional groups is needed.

Steric effects should lead in general to a decrease of the reactivity of the remaining functional groups after other groups in the unit have reacted due to a poorer accessibility of the functional groups. Nevertheless, those effects are supposed to be of minor importance for the system studied as the reactive sites in the terephthaloyl chloride are in a *para*-position with respect to each other, while those in the TMS−THPE are separated by two aromatic rings. To understand the influence of electronic effects on the reactivities, the reaction mechanisms have to be considered (Figure 4). In any case, the concentration of the intermediate phenolate ion has an influence on the reactivity of the corresponding B group. The influence of the addition of the phenolate to the acid chloride on the overall reactivity however is uncertain and depends on the relative reactivity of the phenolate formed. We supposed that in the reaction medium used, the phenolate may form a kind of contact ion pair with the catalyst or may even be protonated. In this case the overall reactivity for the reaction of an A with a B group would be controlled by the stability of the phenolate formed as well as by the reactivity of the acid chloride.

The reactivity of the acid chloride generally depends on the electrophilicity of the carbonyl carbon. As the aromatic ring can easily transmit electronic influences, the electrophilicity depends on the type of functional group present in the *para*-position. Hammett constants σ_p allow a comparison of the electron-withdrawing character of different functional groups on an aromatic ring. The larger σ_p is, the more pronounced is the electron-withdrawing character of the group. A comparison of the Hammett constants that are $\sigma_p = 0.61$ for the acid chloride compared to $\sigma_p = 0.44$ for the phenyl ester[34] yields a stronger electron attraction exerted by the acid chloride. This means that the acid chloride groups in A_2 are more electrophilic and reactive to the phenolate than that in Aa, which corresponds to the observed kinetic situation. Furthermore, we could confirm this reactivity by the comparison with a model reaction, the reaction of (4-ethylphenoxy)trimethylsilane with terephthaloyl chloride. For this reaction, the relative reactivities could be determined from the relative concentrations of the low molecular weight products at complete conversion of the A groups. We found a decrease of the reactivity of the second A group to 42% of the reactivity of the first one, which is quite close to the ratio of the values in the first and second row of the matrices in Table 3, i.e., the reactivity ratios found in the polymerization.

The interpretation is more difficult for the B groups, where an independent reactivity due to the separation of the functional groups by several bonds including a sp^3-hybridized carbon is expected. Steric effects should be weak and have, if at all, rather a retarding effect. A similar AB_2 type molecule, 4,4-bis(4′-hydroxyphenyl)pentanoic acid, showed an independent reactivity of the two B groups.[23] The increase of the reactivity might be explained by electronic interactions between the aromatic systems through space.

Development of the DB with Stepwise Addition of the $A_2 + B_3$ Monomer Mixture. As already shown for AB_2 monomers the DB can be increased by the slow addition of the monomer.[19] Schmaljohann and Voit predicted a similar increase of the DB for $A_2 + B_3$ systems if the B_3 monomer or a mixture of the monomers are added before gelation.[28] On the basis of this prediction, the development of the DB was studied experimentally for the case of a simultaneous addition of both monomers. The resulting development of the DB is shown in Figure 11. It should be noted that the addition of monomer mixture decreases the measured conversion of the system.

One clearly observes an enhancement of the DB for equal conversions of functional groups after the first addition of a monomer mixture. A comparison with a simulation, using the $K_{3:2}$ matrix obtained from the fitting of the A_2:B_3 = 3:2 case (Table 3), shows an excellent agreement between experiment and simulation up to just before the second addition. However, after a second addition, the DB did not increase further in contradiction to the predictions obtained by the simulation. After the third addition, it was not possible anymore to obtain a homogeneous melt, so that the kinetics could not be continued.

A possible explanation of the behavior after the second addition would be the formation of inhomogeneities on a microscopic scale, for example the unreacted monomer being not completely soluble in the preformed polymers. Furthermore, it is possible that the system already started to cross-link in minor fractions leading to an error in the determination of the relative concentrations of the structural units.

Thus, it is in general possible to enhance the DB by sequential addition of monomer for $A_2 + B_3$ systems, too, as it was predicted by the simulation. But at the same time the gel points of those systems are not only related to the overall conversion of the functional groups but rather depend on the parts of the system that have the highest molecular weights and thus on the history of the system. By adding monomer mixture to a reaction mixture that is close to cross-linking, the overall conversion will be decreased, even though the formation of a few bonds will be sufficient to finally cross-link the system. Furthermore, the system seems to be less homogeneous. For these reasons results obtained solely from the simulation should be interpreted with care.

(b) Polymerization of A_2 Monomer AA and B_3 Monomer THPE. The combination of adipic acid as A_2 monomer with THPE as B_3 monomer was chosen because of the good separation of the carboxylic acid groups in the adipic acid, which was supposed to lead to an independent reactivity. For several other reasons as the longer reaction time, the impact of side

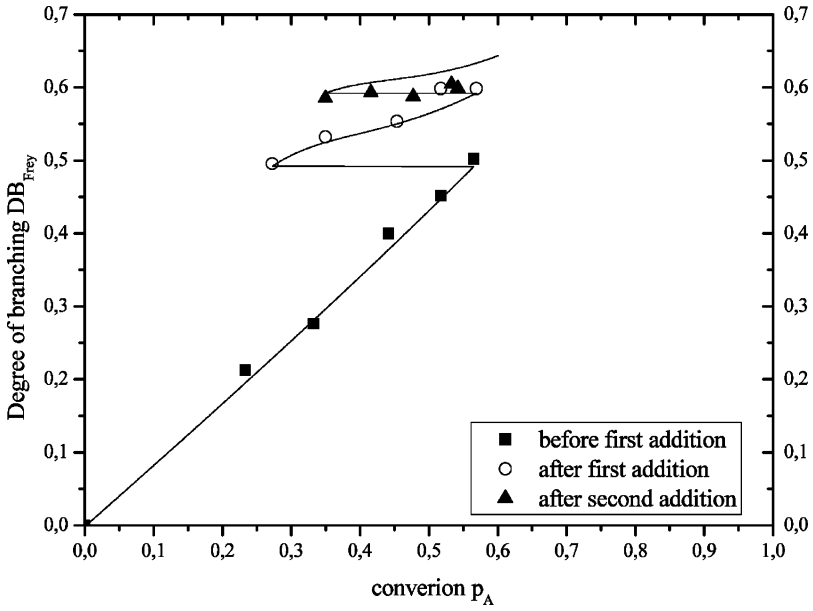

Figure 11. Development of the degree of branching DB_{Frey} as a function of the conversion of the A groups p_A by stepwise addition of the TCl/TMS−THPE monomer mixture (3:2). The points are the experimental values up to the first addition, after the first addition and after the second addition respectively. The line was obtained by a simulation with addition of monomer mixture and the matrix of rate constants fitted for the ratio A_2:B_3 = 3:2 (see Table 3).

reactions, and volatilization of adipic acid, as will be further detailed in the discussion, this system was not as well suited for the kinetic study as the system described above, and so only the monomer ratio 3:2 was studied.

As in the case of the system described prior to this, it was possible to follow quantitatively the development of the structural units based on ^{1}H NMR. A comprehensive ^{1}H and ^{13}C signal assignment was achieved by combined analysis of one- and two-dimensional ^{1}H and ^{13}C NMR spectra (see Supporting Information). We do not describe this analysis in detail but discuss some results with respect to the quantitative structural analysis, which is based on the ^{1}H NMR spectra (Figure 5c). The signals of the methyl groups of B_2b, Bb_2, and b_3 structural units and of the B_3 monomer, which are used to calculate the relative contents, are closer together than in the system described above. In order to eliminate possible falsifications of the relative concentrations due to overlap of the signals at high conversions, the integrals were determined by deconvolution. In the case of the Aa and a_2 units, the signals of the protons $H^{11'}$ are close to the residual solvent signal, while those *o*f H^{11} overlap for the A_2 and Aa units. As a consequence all the concentrations were determined from the signals of the protons H^{12} and $H^{12'}$, which did not interfere with other signals. The conversion of A groups was determined as the ratio of the integral over the signals belonging to the reacted a groups ($H^{12'}$ region from 1.61 to 1.8 ppm) to the total integral of protons H^{12} and $H^{12'}$.

Several factors contribute to relative changes of the ratio of the overall concentration of the A_2 monomer and the structural units derived from it to the overall concentration of the B_3 monomer and the resulting structural units: as for the system described above part of the A_2 monomer is lost by volatilization. Furthermore, the melt obtained in the beginning is not homogeneous and a part of the B_3 monomer, having a melting point of 247 °C, remains initially undissolved. With the system getting homogeneous after a conversion of about 10%, this part is also incorporated in the homogeneous melt.

At the conditions present for this reaction, the THPE partially decomposes according to Figure 12. The corresponding products

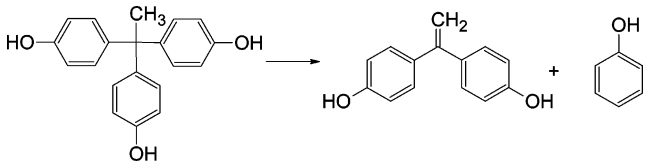

Figure 12. Side reaction of the THPE in the system adipic acid/THPE leading to a bisphenol and phenol.

could be identified by NMR, leading to the conclusion that at least the resulting bisphenol participates in the polymerization reaction, too, acting as a B_2 monomer. The concentration of the byproducts increases during most of the reaction up to at least p_A = 60%. At this point about 7% of the original amount of B_3 monomer has reacted in the side reaction. Even though the byproduct could be distinguished by NMR spectroscopy, the experimental error in the determination of the concentration of the byproduct and its derivatives is so large, that a detailed quantitative analysis of those products would be merely speculative.

These three processes influence the ratio of bifunctional to trifunctional units in different ways and directions. The loss of A_2 monomer was already discussed above. The slower melting of a part of the B_3 monomer leads to a slight increase of the B_3 concentration during the early phase of the experiment, resulting in a further decrease of the A_2:B_3 ratio. Both processes only take place during the early phase of the reaction, and at about 30% conversion, a relatively constant value of the A_2:B_3 ratio about 8% below the starting value is reached (see Supporting Information). The side reaction leads to a faster decrease of the concentration of the B_3 monomer and to lesser concentrations of the other trifunctional units. As one of the byproducts participates itself in the reaction, the side reaction has only a minor effect on the concentration of the B groups.

Development of the Structural Units and of the Degree of Branching with Conversion for the AA /THPE System and Its Simulation by Relative Rate Constants. The development of the concentrations of the different structural units are presented in Figure 13 (see also Supporting Information). They have been normalized to the overall concentration of bifunctional

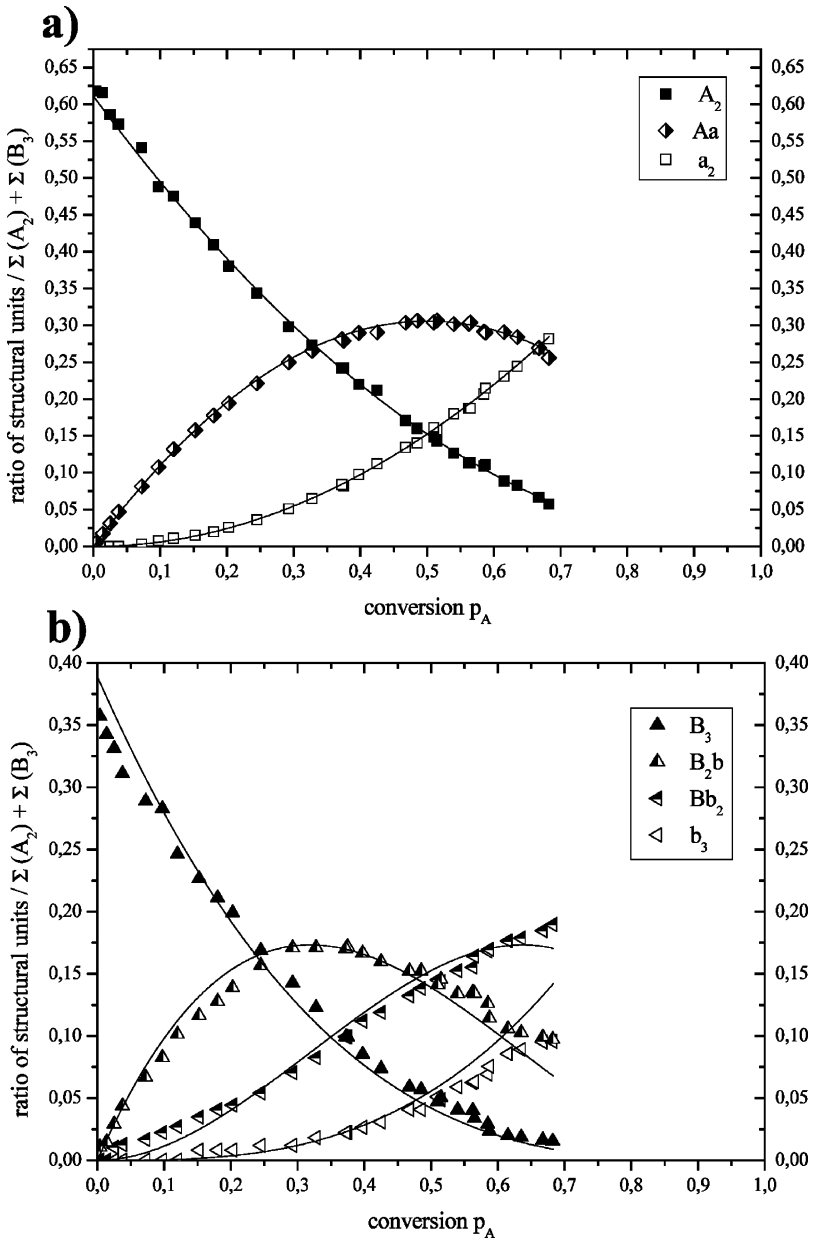

Figure 13. Comparison of experimental data and simulation (a) for the A_2, Aa, and a_2 units and (b) for the B_3, B_2b, Bb_2, and b_3 units of the system AA/THPE (3:2). The symbols give the experimental data for the structural units as a function of conversion p_A, the lines give the data obtained from a simulation with the ideal matrix **K**(1). All data are normalized to the sum of all structural units.

units, that is A_2, Aa, and a_2, and trifunctional units, that is B_3, B_2b, Bb_2, and b_3. The side products have not been included in the normalization, so that the curves are more easily comparable to those described above. As the reaction became extremely slow at higher conversions, the gel point was not reached, and the polymerization was stopped at a conversion of 68% reached after 90 h.

The differences between the two systems studied are especially highlighted by the comparison of the development of the degree of branching for an equal starting ratio A_2:B_3, i. e. 3:2. The DB of the system composed of adipic acid and THPE increases more slowly (and reaches with about 53% a lower final value ($p_A = 68\%$) as the TCl−TMS−THPE system (61%) at same conversion ($p_A = 69\%$) described before.

Comparison of the experimental data with a simulation based on an equal and independent reactivity of the functional groups, i.e., with the **K**(1) matrix, shows a very good agreement for the bifunctional units (Figure 13a). For the trifunctional units the agreement is less pronounced (Figure 13b). Especially the experimental data points for the B_2b and b_3 units seem to be displaced to higher conversions in comparison to the simulation. The relative content of Bb_2 units seems to be too high in the beginning. This is probably due to the superposition of the corresponding signal with a ^{13}C satellite of DMSO-d_6, leading to a slight overestimation of the concentration, which is especially pronounced for a small Bb_2 signal.

Optimization of the rate constants yielded a slightly positive substitution effect for the trifunctional units. The comparison of the obtained curves however did not show a visible improvement of the agreement between experiment and simulation. The formed byproduct also takes part in the reaction and leads to a relative lowering of the conversion of the A groups with respect to the trifunctional B units. This could explain the shift of the curves of the B_2b and b_3 units to higher conversions.

It thus can be concluded, that the reactivities of the A groups in this system are really equal and practically independent. The same can be said of the reactivities of the B groups in the limits of the experimental error. This together with the shift of the

curves to higher conversions explains the lower DB as compared to the system discussed prior.

Conclusions

For two $A_2 + B_3$ systems, the relative concentrations of the different structural units could be determined by ^{1}H NMR spectroscopy at different conversions before gelation. Computer simulation based on a theoretical model developed earlier in our group led to a good fit of the experimental data to the simulated curves and, finally, to a set of relative rate constants for the different reaction steps.

For the system consisting of terephthaloyl chloride and TMS−THPE a nonideal kinetic situation was observed and could be well reproduced for different starting ratios of the monomers. We found that the stability of the phenolate formed as well as the electrophility of the acid chloride have an influence on the relative reaction rates. The relatively small effect of the stability of the phenolate on the relative reactivities of B groups is due to the good separation of the functional groups in the B_3 monomer. The effect of the acid chloride was bigger and could qualitatively be explained by substitution effects supported by Hammett parameters.

The effect of increasing degree of branching by stepwise addition of the monomer mixture could be established also for the $A_2 + B_3$ system. Comparison of the experimental results with the simulation using the parameters obtained for this system showed a very good agreement up to the second addition. After the second addition the simulated further increase of the DB was not observed experimentally. Possible reasons for this may be inhomogeneities in the reaction milieu or a beginning of the gelation.

The system composed of adipic acid and THPE had some shortcomings especially a shift in the ratio of the two components and part of the B_3 monomer was consumed in a side reaction. Comparison of the experimental data with the simulation gave, however, a good agreement for the bifunctional units and an acceptable agreement for the trifunctional units. It could be shown that the kinetic situation is ideal for the A_2 units and in the frame of the experimental errors also ideal for the B_3 monomer.

The usefulness of the kinetic model and the simulations based thereon for the analysis of hyperbranched polymerizations based on $A_2 + B_3$ systems could be shown. An interesting expansion of the simulation could be toward the prediction of the point of gelation for nonideal polymerizations and for the stepwise addition of one or both of the monomers.

Supporting Information Available: Text and tables giving complete ^{1}H and ^{13}C NMR signal assignments and figures showing selected 1D and 2D spectra for the TCl/TMS−THPE and for the AA/THPE system, text giving a detailed description of the kinetic evaluation in matrix notation, and figures giving the development of the structural units with conversion for the TCl/TMS−THPE and for the AA/THPE. This material is available free of charge via the Internet at http://pubs.acs.org.

References and Notes

(1) Tomalia, D. T.; Fréchet, J. M. J. *J. Polym. Sci., Part A: Polym. Chem.* **2002**, *40*, 2719−2728.
(2) Jikei, M.; Kakimoto, M. *Prog. Polym. Sci.* **2001**, *26*, 1233−1285.
(3) Voit, B. *J. Polym. Sci., Part A: Polym. Chem.* **2000**, *38*, 2505−2525.
(4) Voit, B. *J. Polym. Sci., Part A: Polym. Chem.* **2005**, *43*, 2679−2699.
(5) Gao, C.; Yan, D. *Prog. Polym. Sci.* **2004**, *29*, 183−275.
(6) Yates, C. R.; Hayes, W. *Eur. Polym. J.* **2004**, *40*, 1257−1281.
(7) Kim, Y. H. *J. Polym. Sci., Part A: Polym. Chem.* **1998**, *36*, 1685−1698.
(8) Fréchet, J. M. J.; Hawker, C. J. Synthesis and Properties of Dendrimers and Hyperbranched Polymers. In *Comprehensive Polymer Science*; Aggarwal, S. L., Russo, S., Eds.; Elsevier Science Ltd.: Oxford, England, 1996; 2nd Supplement, p 71 ff.
(9) Fréchet, J. M. J.; Henmi, H.; Gitsov, I.; Aoshima, S.; Leduc, M. R.; Grubbs, R. B. *Science* **1995**, *269*, 1080−1083.
(10) Chang, H.-T.; Fréchet, J. M. J. *J. Am. Chem. Soc.* **1999**, *121*, 2313−2314.
(11) Sunder, A.; Hanselmann, R.; Frey, H.; Mülhaupt, R. *Macromolecules* **1999**, *32*, 4240−4246.
(12) Magnusson, H.; Malmström, E.; Hult, A. *Macromol. Rapid Commun.* **1999**, *20*, 453−457.
(13) (a) Flory, P. J. *J. Am. Chem. Soc.* **1941**, *63*, 3083−3090. (b) Flory, P. J. *J. Am. Chem. Soc.* **1941**, *63*, 3091−3096. (c) Flory, P. J. *J. Am. Chem. Soc.* **1941**, *63*, 3096−3100.
(14) Kricheldorf, H. R.; Schwarz, G. *Macromol. Rapid Commun.* **2003**, *24*, 359−381.
(15) Kuchanov, S.; Slot, H.; Stroeks, A. *Prog. Polym. Sci.* **2004**, *29*, 563−633.
(16) Stockmayer, W. H. *J. Chem. Phys.* **1943**, *11*, 45−55.
(17) Beginn, U.; Drohmann, C.; Möller, M. *Macromolecules* **1997**, *30*, 4112−4116.
(18) (a) Müller, A. H. E.; Yan, D.; Wulkow, M. *Macromolecules* **1997**, *30*, 7015−7023. (b) Yan, D.; Müller, A. H. E.; Matyjaszewski, K. *Macromolecules* **1997**, *30*, 7024−7033. (c) Matyjaszewski, K.; Gaynor, S. G.; Müller, A. H. E. *Macromolecules* **1997**, *30*, 7034−7041.
(19) Frey, H. *Acta Polym.* **1997**, *48*, 298−309.
(20) Malmström, E.; Hult, A. *Macromolecules* **1996**, *29*, 1222−1228.
(21) Galina, H.; Lechowicz, J. B.; Kaczmarski, K. *Macromol. Theory Simul.* **2001**, *10*, 174−178.
(22) McCoy, B. J. *J. Colloid Interface Sci.* **1999**, *216*, 235−241.
(23) Schmaljohann, D.; Komber, H.; Voit, B. *Acta Polym.* **1999**, *50*, 196−204.
(24) Schmaljohann, D.; Komber, H.; Voit, B.; Barratt, J. G.; Appelhans, D. *Macromolecules* **2003**, *36*, 97−108.
(25) Schmaljohann, D.; Barratt, J. G.; Komber, H.; Voit, B. *Macromolecules* **2000**, *33*, 6284−6294.
(26) Dusek, K.; Duskova-Smrckova, M.; Voit, B. *Polymer* **2005**, *46*, 4265−4282.
(27) Unal, S.; Oguz, C.; Yilgor, E.; Gallivan, M.; Long, T. E.; Yilgor, I. *Polymer* **2005**, *46*, 4533−4543.
(28) Schmaljohann, D.; Voit, B. *Macromol. Theory Simul.* **2003**, *12*, 679−689.
(29) The nomenclature used here differs from the one introduced in ref 28. So, e.g., the unit named B1 in ref 28 is B_3 here, and B4 is called b_3 here.
(30) (a) Mandolini, L. *Adv. Phys. Org. Chem.* **1986**, *22*, 1−110. (b) Ercolani, G.; Mandolini, L.; Mencarelli, P. *Macromolecules* **1988**, *21*, 1241−1246.
(31) (a) Kricheldorf, H. R.; Hobzova, R.; Vakhtangishvili, L.; Schwarz, G. *Macromolecules* **2005**, *38*, 4630−4637. (b) Kricheldorf, H. R.; Vakhtangishvili, L.; Schwarz, G. *J. Polym. Sci., Part A: Polym. Chem.* **2004**, *42*, 5725−5735. (c) Kricheldorf, H. R.; Fritsch, D.; Vakhtangishvili, L.; Schwarz, G. *Macromolecules* **2003**, *36*, 4337−4344.
(32) (a) Dusek, K.; Somvarsky, J.; Smrckova, M.; Simonsick, W. J., Jr.; Wilczek, L. *Polym. Bull. (Berlin)* **1999**, *42*, 489−496. (b) Cameron, C.; Fawcett, A. H.; Hetherington, C. R.; Mee, R. A. W.; McBride, F. V. *Macromolecules* **2000**, *33*, 6551−6568.
(33) Galina, H.; Lechowicz, J. B.; Potoczek, M. *Macromol. Symp.* **2003**, *200*, 169−180.
(34) Kricheldorf, H. R.; Schwarz, G. *Makromol. Chem.* **1983**, *184*, 475−496.
(35) Hansch, C.; Leo, A.; Taft, R. W. *Chem. Rev.* **1991**, *91*, 165−195.

MA070812G